JOURNAL OF THE KOREAN ASTRONOMICAL SOCIETY
36: 21 ~ 31, 2003

THERMAL MODELS AND FAR INFRARED EMISSION OF ASTEROIDS

SAM KIM[1], HYUNG MOK LEE[1,2], TAKAO NAKAGAWA[2] AND SUNAO HASEGAWA[2]
[1] Astronomy Program, School of Earth and Environmental Sciences, Seoul National University, Korea
[2]Institute of Space and Astronautical Science, 3-1-1 Yoshinodai, Sagamihara, Kanagawa 229-8510, Japan
e-mail: dhyan@astro.snu.ac.kr, hmlee@astro.snu.ac.kr, nakagawa@ir.isas.ac.jp, hasegawa@planeta.sci.isas.ac.jp
(Received Feb. 10, 2003; Accepted Mar. 21, 2003)

ABSTRACT

ASTRO-F/FIS will carry out all sky survey in the wavelength from 50 to 200 μm. At far infrared, stars and galaxies may not be good calibration sources because the IR fluxes could be sensitive to the dust shell of stars and star formation activities of galaxies. On the other hand, asteroids could be good calibration sources at far infrared because of rather simple spectral energy distribution. Recent progresses in thermal models for asteroids enable us to calculate the far infrared flux fairly accurately. We have derived the Bond albedos and diameters for 559 asteroids based on the IRAS and ground based optical data. Using these thermal parameters and standard thermal model, we have calculated the spectral energy distributions of asteroids from 10 to 200 μm. We have found that more than 70% of our sample asteroids have flux errors less than 10% within the context of the best fitting thermal models. In order to assess flux uncertainties due to model parameters, we have computed SEDs by varing external parameters such as emissivity, beaming parameter and phase integral. We have found that about 100 asteroids can be modeled to be better than 5.8% of flux uncertainties. The systematic effects due to uncertainties in phase integral are not so important.

Key words : asteroids – thermal models – infrared

I. INTRODUCTION

Flux calibration is one of the most important parts in astronomical observations. In the optical wavelength bands, the absolute fluxes of many standard stars have been accurately measured repeatedly with standard filter systems. Other objects can be calibrated by comparing the measured flux with those of standard sources.

However, in the far-infrared bands (FIR), measuring and determining the absolute flux are not straightforward. Starburst galaxies and late type stars emit relatively strong radiation in the FIR bands. The fluxes of these objects, however, are difficult to model, because the FIR fluxes are sensitive to the environments. For example, the spectral energy distributions (SED) of late type stars in far infrared are sensitive to the existence of circumstellar envelope. Galaxies are also difficult to use a calibration sources because similar morphological type galaxues exhibit rather diverse SEDs in the FIR bands depending on their star formation activities.

The infrared all sky survey mission of Infrared Astronomical Satellite (IRAS) had four photometric bands: 12, 25, 60 and 100 μm. The absolute calibrator of the 12 μm band photometry was a late type star, α Tau, whose flux was carefully measured from ground based observations at 10.6 μm (Rieke, Lebofsky, & Low 1985). The absolute flux at 12 μm of α Tau was derived by extrapolating from the measured fluxes at 10.6 μm. assuming that this star is a black-body.

The calibration at 25 and 60 μm bands has been done using stellar models. The solar photometry (Vernazza, Avrett, & Loeser 1976) as well as stellar model calculations (e.g., Kurucz 1979) showed that the colors, e.g., [12 μm]-[25 μm] and [25 μm]-[60 μm], are similar for stars with wide range of various temperatures. The same color can be applied to a number of stars that have been well measured by IRAS, and that do not show any obvious excess at 60 μm relative to α Tau, in order to obtain fluxes at 25 and 60 μm. These stars were used as calibration sources at 25 and 60 μm.

The calibration at 100 μm band was carried out using asteroids. Three asteroids (Hygiea, Europa and Bamberga) were observed at eight occasions with the pointed mode of IRAS. The color temperatures at 25 and 60 μm bands were applied to those at 60 and 100 μm in order to derive the fluxes at 100 μm band. The averages of 100 μm fluxes of these asteroids were used for absolute calibration in this band.

ASTRO-F by Institute of Space and Astronautical Science (ISAS) of Japan will carry out extensive observations in near to far infrared bands (e.g., Murakami 1998). Far Infrared Surveyor (FIS), one of the focal plane instruments of ASTRO-F, will survey the entire sky in four bands in the wavelength range of 50~ 200 μm. Since ASTRO-F/FIS will survey with longer wavelength than that of IRAS, the flux calibration method will be different from that of IRAS.

Although IRAS used asteroids for calibration of 100

Corresponding Author: H. M. Lee

μm band only, asteroids can be calibration sources for the entire bands of ASTRO-F. The main advantage of using asteroids is the absence of the atmospheres which could cause rather complex emission features. Since there is no internal energy source and contribution from the reflected solar light is negligible, the FIR emission from the asteroid is mainly due to thermal emission (e.g., Hasegawa 1998). Recent advances in thermal models of asteroids allow accurate estimates of temperature distribution over the surface (e.g., Müller & Lagerros 1998, 2002).

The main purpose of this paper is to calculate the spectral energy distribution (SED) of many asteroids in the context of rather simple thermal models. Using IRAS data as well as recent ground based data, we attempt to find the best parameters for thermal models of individual asteroids. We then assess the possible calibration uncertainties originated from uncertainties in various model parameters as well as the model itself.

This paper is organized as follows. We give brief introduction to the asteroids in general in §2. The procedure of finding the model parameters using various data is described in §3. We present the best-fitting thermal parameters in §4, and discuss the calibration uncertainties in §5. The final section summarizes the major findings of this paper.

II. PROPERTIES OF ASTEROIDS

Asteroids are important objects for studying the origin of the solar system, since they have experienced very little geological and thermal evolution. Even though the distribution of size and geometric albedo of asteroids are crucial information for studying the solar system, it is not easy to obtain them due to following reasons. The angular diameters of asteroids do not exceed 0.8 arcsec even for the largest asteroid, Ceres. Majority of asteroids are smaller than 0.01 arcsec. Direct determination of the diameters has been possible only for a small number of big asteroids. Adaptive optics, speckle interferometry, and Hubble Space Telescope have been used to measure the sizes of small number of asteroids (see references in Hasegawa 1998).

Another method of estimating diameter is to use the thermal infrared radiation from the asteroids. The radiation of the asteroids in the wavelength bands shorter than 2.5 μm is dominated by the reflected solar radiation, while the thermal radiation dominates in the wavelength bands longer than 5 μm. The transition between thermal and reflected emission occurs at 2.5 $\sim$ 5 μm. The critical transition wavelength depends on various parameters such as albedo, heliocentric distance and other thermal parameters of the asteroids (Lebofsky & Spencer 1989). We can safely assume that the FIR emission in the ASTRO-F/FIS bands is completely dominated by thermal radiation since shortest wavelength covered by this instrument is 50 μm.

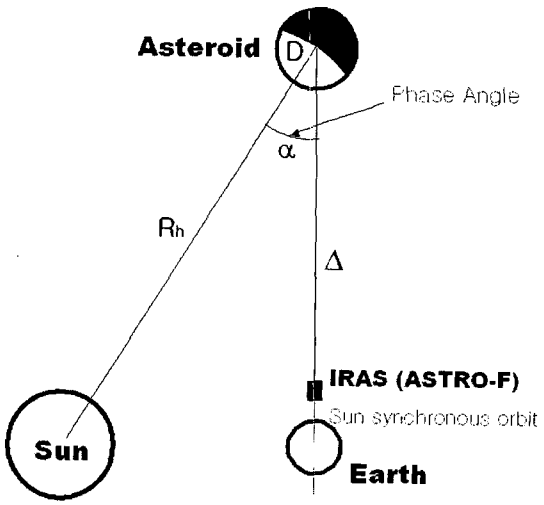

Fig. 1.— Typical geometry of the IRAS (or ASTRO-F) observations of asteroids. The solar elongation angle (Sun-Earth-Asteroid angle) is generally 90°. Here, α is the phase angle, D is the size of asteroid, and R_h and Δ are the heliocentric and geocentric distances, respectively.

(a) Thermal Parameters of Asteroid

For the further discussion of thermal emission and thermal structure of asteroids, we first define several physical parameters for the observations of asteroids (See Fig. 1). In Sun-asteroid-Earth positional geometry, we also have to know about the size (D), heliocentric distance (R_h) and the geocentric distance (Δ) of the asteroid.

We will examine the intrinsic properties of the asteroids, i.e., Bond albedo and diamter. The Bond albedo, A_b, is the fraction of light reflected by a disk illuminated and observed perpendicularly. This value depends on the spectrum of the illuminating source. The 'bolometric Bond albedo' expresses the albedo over the entire spectral range. Since the asteroid is not a disk, the actual fraction of the reflected light is different from the Bond albedo. The fraction of reflected light to the direction to the illuminating source of an arbitrary shaped body is called 'geometric albedo', and denoted by p. Therefore, the average reflected flux F (normal to the illuminating source) and illuminating flux s are related by $F = ps$. The relationship between geometric and Bond albedos is usually expressed as

$$A_b = qp, \tag{1}$$

where q is called phase integral. For a spherical body whose albedo does not depend on the wavelength, q is 2/3. If the albedo depends on the wavelengh and the shape of asteroid is not spherical, actual value of q differs from 2/3. The geometric albedo (p) is defined

when asteroid is located at zero phase angle ($\alpha = 0°$). Practically, measurements of albedos at several different phases are used to extract the value of p. Comprehensive model has been developed to determine p from a series of ground based observations.

Before we calculate thermal emission of the asteroid, we have to determine the geometric albedo (p) and the diameter (D), using the relationship between the visual magnitude and the thermal flux. Visual magnitude is the function of the asteroid's diameter and the geometic albedo in visual band. The brightness of the asteroid depends on the phase angle α and the distance. The dependency of the V magnitude at solar phase angle, the absolute magnitude $H(\alpha)$ (magnitude measured at the unit heliocentric and geocentric distances), can be expressed by

$$H(\alpha) = H - 2.5 \log [(1 - G)\Phi_1(\alpha) + G\Phi_2(\alpha)], \quad (2)$$

where H is the absolute magnitude at α=0°. The two functions Φ_1 and Φ_2 are two specified phase functions that are normalized to 1 at α=0°. Therefore the phase curve of a given asteroid is decomposed into two phase functions Φ_1 and Φ_2 in the ratios $(1 - G) : G$. These functions Φ_1 and Φ_2 have quite complex shape, and are described in the appendix of Bowell et al. (1989). The fitting parameter G is the slope parameter of the phase curve. This parameter can be obtained by a series of observations in V-band for a given asteroids at several different phase angles. The phase integral of the asteroid can be approximated as

$$q = 0.290 + 0.684G. \quad (3)$$

Most reflected light observations are reported in the broadband Johnson V filter. Since most of solar radiation comes through V-band wavelengths, we may assume that

$$p_v = p, \quad (4)$$

where p_v is the albedo at V band which is centered at 0.56 μm. The error in the determination of A_b caused by this assumption is known to be only a few % which is smaller than other errors.

Since the flux of an asteroid at the phase angle α=0° at the heliocentric distance of 1 AU is

$$F_v = \frac{\pi (D/2)^2 p_v S_\odot}{4\pi \Delta^2}, \quad (5)$$

the absolute magnitude H becomes

$$H = -2.5 \log(D^2) - 2.5 \log(p_v) + const. \quad (6)$$

The constant can be fixed with precise definition of H and the result is conveniently expressed as follows

$$\log D = 3.1236 - 0.5 \log(p_v) - 0.2H, \quad (7)$$

where D is in units of meter. The ground based observations only give H and G data. Using eq. (3), one can obtain the value of q. Theree other parameters D, p_v and H are related by eq. (7). Therefore, p_v is the only free parameter to be determined (aside from external thermal parameter, ϵ and η which can be separately measured for a small number of asteroids as described below.)

Since asteroids are not perfect black-body sources, we need to know the emissivity (ϵ) to compute the thermal flux from the asteroids. We assume that the emissivity ϵ is wavelength-independent in the FIR bands where the thermal emission is important. The typical value of ϵ is 0.9 (Lebofsky et al. 1986; Lebofsky & Spencer 1989). However, recent study of ϵ based on near infrared to submillimeter band of Ceres, Pallas and Vesta indicates that ϵ depends slightly on the wavelengths (Müller & Lagerros 1998). The combined results of Ceres and Pallas show that the value ϵ is about 1 at 20 μm, and drops to 0.8 at around 200 μm. For the case of Pallas, the FIR emissivity drops to 0.6. We adopt canonical value of 0.9 in the present study, but examined sensitivities of thermal model parameters on ϵ (see §5).

The thermal emission from surface of the Moon is anisotropic, because of the irregularity of the lunar surface. The depressed regions (e.g., sea areas) radiate more thermal radiation toward the direction of the Sun because these regions can absorb more radiation from the surrounding walls. Therefore, the subsolar temperature (where the altitude of the Sun is 90°), tends to be higher than the predicted value based on the simple equilibrium estimates. Such effect can be approximated by introducing the *beaming* factor, η such that

$$T^4_{ss,obs} = \eta T^4_{ss,theory} \quad (8)$$

where the subscript *ss* represents the 'subsolar point', and *obs* and *theory* mean the observed, and theoretical values, respectively. Because of the beaming toward the direction of the Sun, the temperature gradient toward the limb is less than expected from the simple equilbrium estimates. The beaming factor tends to enhance the flux at zero phase angle. In order to keep the energy conserved, the flux should decrease more rapidly with increasing phase angle than the predicted results. In order to compensate such enhancement, the flux at non-zero phase angle can be reduced with phase angle by a factor proportional to α such that $F(\alpha) = F(0) \exp(-\tau\alpha)$, where τ is the reduction factor per degree. Since the brightnesses are usually expressed in magnitude in astronomy, it is sometimes more convenient to define 'thermal coefficient', β_E, in units of magnitude per degree: $\beta_E = 2.5\tau_\lambda \log e = 1.086\tau_\lambda$. This coefficient is in the range between 0.005 and 0.017 mag deg^{-1}. We adopted the average value of 0.01 mag deg^{-1} (Lebofsky & Spencer 1989) in the present study. Since the assumption that the reduction of flux is proportional to the phase angle does not have any concrete ground, this approximation could lead to large errors at large phase angles.

(b) Thermal Balance on Asteroids

Three basic thermal models have been developed for infrared observational method. In §2(c) these models are described in detail. These methods assume that the body is in equilibrium state between the absorbed sunlight and the thermal emission. In the lack of internal energy source and complicated effects of atmospheres, the thermal balance in asteroids can be easily modelled.

For simplicity, the asteroid is assumed to be spherical. The global energy balance equation is

$$\pi(D/2)^2(1-A_b)S/R_h^2 = \eta(D/2)^2 \int\int \epsilon\sigma T^4(\theta,\phi)\sin(\theta)d\theta d\phi, \quad (9)$$

where S is the solar flux at unit distance (usually at 1 AU), σ is the Stephan-Boltzman constant and T is the surface temperature. The surface temperature T depends on the position on the asteroid. We use the spherical coordinate as shown in Fig. 2. The equatorial plane is defined as the orbital plane of the asteroid and the latitude angle, θ is measured from the north pole. The longitude angle, ϕ is measured from subsolar point. The global balance shown in eq. (9) needs information on the local temperature distribution $T(\theta,\phi)$ which contributes to the thermal flux distribution shape. We have to rely on specific thermal model in order to specify the surface temperature distribution.

(c) Thermal Models

The temperature on the surface of asteroid is determined by rather complicated processes: the heat balance between the solar irradiation and the thermal emission, and the heat transfer from hot region to cool region on the surface. The complex geometry of the asteroid causes further complication. Sophiscated models that take some of these effects into account are available for well observed asteroids (see, for example, Müller & Lagerros 2002). Such thermophysical models are beyond the scope of this paper since our purpose is to examine the thermal properties of astroids in general. We concentrate rather simple models which are described below.

i) Standard Thermal Model

Standard Thermal Model (STM; Morrison & Lebofsky 1979) assumes that the local thermal balance is achieved without heat conduction on the surface of the asteroids as illustrated in Fig. 2. This model can be applied to the asteroids with very slow rotation or with very low thermal inertia. Surface temperature of the STM for an airless body becomes

$$T(\theta,\phi) = \left[\frac{(1-A_b)S}{\eta\epsilon\sigma R_h^2}\sin(\theta)\cos(\phi)\right]^{1/4}. \quad (10)$$

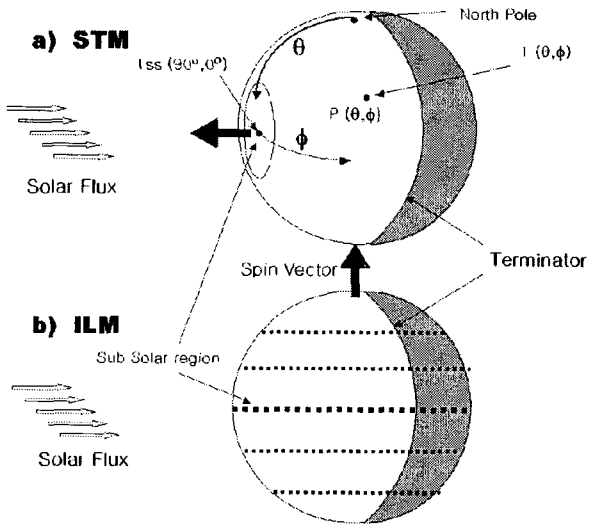

Fig. 2.— Illustration of the two simple thermal models and geometry of asteroid. θ and ϕ are the latitude and the longitude in spherical coordinates, respectively. (a) The standard thermal model (or non-rotating model). The temperature depends only on the incidence angle of solar ray. (b) The isothermal latitude model (or fast rotating model). The temperature depends only on latitude θ.

The normal beaming, η of the STM is estimated to be 0.756 from the study of Ceres and Pallas (Lebofsky et al. 1986). We will examine the sensitivity of thermal properties on η in §5 .

ii) Isothermal Latitude Model

Isothermal latitude model (ILM) assumes that the temperature depends only on the latitude θ. ILM can be applied to asteroids with the extremely high thermal inertia, or rapidly rotating asteroids (Lebofsky & Spencer 1989). Surface temperature of the ILM is given by

$$T(\theta) = \left[\frac{(1-A_b)S}{\pi\epsilon\sigma R_h^2}\sin(\theta)\right]^{1/4}. \quad (11)$$

ILM has been used for deriving thermal structure and albedo and diameters for several earth-approaching asteroids.

iii) Near Earth Asteroid Thermal Model

Another new thermal model for near-earth asteroids (NEATM) was proposed by Harris (1998). This model is identical to STM except for η. The near-earth asteroids have relatively high η. The standard value of η in NEATM is 1.2 while the conventional value for STM is 0.756.

III. DERIVATION OF THERMAL PARAMETERS

Among three thermal models discussed above, STM is known to reproduce the IRAS observations fairly well (Hasegawa 1998). Thus we will use only STM in the present paper. The key parameters of STM in determining the temperature distribution for a given asteroid are A_b, D, η and ϵ, whose values are different for different asteroids. The beaming, η can be estimated by measuring the color temperature in infrared. We adopt the cannonical value, $\eta = 0.756$. The emissivity, ϵ depends on particle size, composition and properties of the surface material. We take a wavelength independent value for the emissivity, $\epsilon = 0.9$. As discussed in §2(a) it is more convenient to use p_v instead of A_b. Assuming $p = p_v$, we can obtain q using the ground based measurement of G by eq. (30. For the ground based measurement data, i.e., H and G, we use the recent compilation of Lowell Observatory's asteroid observation. The compiled asteroid data of Lowell Observatory can be obtained from internet (ftp://ftp.lowell.edu/pub/elgb/astorb.html). In this study we use the data updated in November, 2000.

(a) Data

In this study, we have used *Infrared Astronomical Satellite Asteroid and Comet Survey* (ASAS; Matson 1986) data, which includes IRAS observations from 1811 asteroids with known orbits. Although IRTS (Infrared Telescope in Space) and ISO (Infrared Space Observatory) also observed many asteroids, the number of observed asteroids from the two missions was much smaller than that of IRAS. We only use the sightings covering all four IRAS bands in order to fit with the flux estimated by the thermal model. Among 7000 sightings, about 1500 sightings (for 559 asteroids) of them have four band fluxes.

(b) Fitting Procedure

With assumed values for η and ϵ and measured value of G, we can compute the temperature distribution over the entire asteroid surface if we know $p(= p_v)$. Since we do not know p_v, we can choose a trial value of it and compute $T(\theta, \phi)$. This information can be used to compute the flux at all wavelengths via,

$$\epsilon \pi B_\nu[T(\theta,\phi)]d\nu = \epsilon \frac{2\pi h\nu^3}{c^2} \frac{1}{\exp[h\nu/kT(\theta,\phi)] - 1} d\nu, \quad (12)$$

where B_ν is the Planck function, k is the Boltzmann constant, and h is the Planck constant. In order to compare with the observational data, we compute the monochromatic thermal flux at the Earth by integrating over the entire surface on the asteroid, and by taking into account the beaming factor as follows:

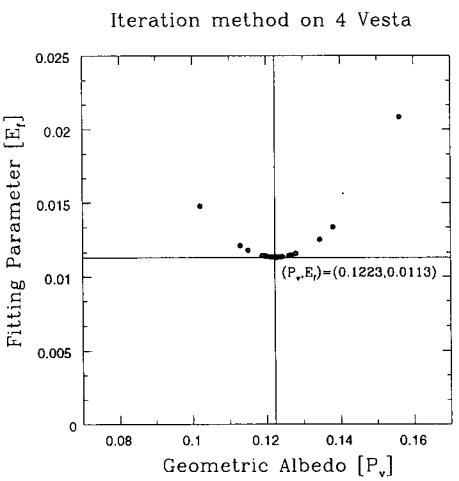

Fig. 3.— An example of least square fitting the quoted flux from IRAS and a model. p_v is geometric albedo. E_f is the *merit function* which is defined by eq. (14). Iteration method was used to find best *intrinsic parameter*, p_v where E_f is minimized.

$$f_\nu = \frac{10^{-0.4\beta_E \alpha}}{\Delta^2} \times \int\int \epsilon B_\nu(T(\theta,\phi))(D/2)^2 \sin\theta \cos(\phi - \alpha) d\Omega, \quad (13)$$

where $d\Omega = \sin\theta d\theta d\phi$. In order to compare with the IRAS data, we need to convert the monochromatic flux into the IRAS flux by performing the convolution over the IRAS response function. This procedure is described in detail in the Appendix. We denote the IRAS flux at $i-$th band as f_i^q and the computed flux as $f_i^{STM,q}$ using STM. Here the superscript q stands for the 'quoted' value. We first calculate $f_i^{STM,q}$ with assumed value of p and evaluate the merit function defined by

$$E_f = \frac{\sum_i \left[(f_i^q - f_i^{STM,q}/f_i^{STM,q} \right]^2 (1/P_i)}{\sum_i (1/P_i)}, \quad (14)$$

$$P_i = \left(\frac{\sigma_i}{f_i^q} \right)^2, \quad (15)$$

and σ_i is the 1-σ uncertainty of the IRAS flux at i-th band. We then take some variation on p and repeat the

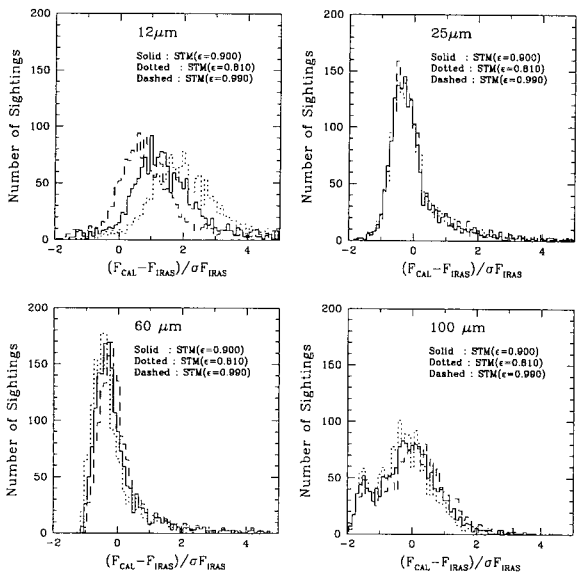

Fig. 4.— Histograms of the quoted flux deviations between IRAS and the model. This figure shows the effect of emissivity, ϵ, on the flux deviation, when it is changed 10% from the conventional value. σF_{IRAS} is the 1-σ flux uncertainty of the IRAS flux. F_{CAL} and F_{IRAS} are the quoted fluxes of IRAS and model. At 12 μm and 100 μm bands, the deviation of model quoted fluxes of the model from those of IRAS are very high.

process again until we reach the minimum value of E_f. This process is illustrated in Fig. 3. We usually find the best fitting p within 10 iterations. Once the best-fitting p is obtained, we can determine the diameter of the asteroid by using eq. (7).

IV. RESULTS

There are about 1500 sightings for 559 asteroids covering four IRAS bands in ASAS database. We made a master database from these sources. We applied our iteration procedure to individual sightings, and obtained multiple values of p (and thus D) for each asteroid that has multiple sightings. We finally assigned p and D to each asteroid by taking averages of these parameters for multiply observed asteroid.

For 1500 sightings we examined the distribution of differences between IRAS and best-fitting model fluxes in Fig. 4. In this figure, we also show the fitting results with different ϵ: 0.99 and 0.81. In general, we find that the model flux does not deviate by more than 2σ of IRAS flux uncertainties from the measure flux. Most of the model predictions lie within 1σ from the observed value. This means that the thermal models reproduce the IRAS data very well. We note that the distributions are wider for 12 μm and 100 μm bands. The dispersion at 100 μm band may be due to rather large measurements errors than the estimated uncertainties. At 12 μm, on the other hand, the thermal model prediction differs systematically from the IRAS data. This might be be due to the contamination of reflected light or complex surface features. We also find that the distribution of flux difference is not symmetric in general. The skewness is very pronounced for 12 μm band where the calculated fluxes are systematically larger than observed fluxes. This may be due to the absorption features in short wavelength band.

The change of emissivity does not have significant effects on the distribution of flux differences except for 12 μm band. The low emissivity tend to increase while the high emissivity tends to decrease the skewness. However, the skewness does not go away even for very large emissivity (ϵ=0.99). We should be able to reduce the skewness by introducing wavelength dependent ϵ, but that is beyond the scope of this work.

(a) Diameters of Asteroids

Diameters of some asteroids have been directly measured, and we compare our derived values with the observed ones. Table 1 lists some example of derived diameters of the previous catalog (Tedesco 1992) in comparison with direct measurements, together with the values determined by Hasegawa (1998). There exists significant differences on the measured diameters depending on the method. Our derived diamaters generally agree very well with the measured diameters. Most of our estimates differ by only up to 4% in diameters. Hasegawa (1998) made a significant improvement in diameter estimates by adopting improved data for H and G. Our method is similar to that of Hasegawa, we used 100 μ data which were omitted byR Hasegawa because of large uncertainties of fluxes in this wavelength band. In this table we also listed the diameters using somewhat smaller values of beaming, η. The standard value was 0.756, but we find that the smaller values of η provide slightly better estimates of D. Our estimates tend to be larger than the previous estimates, which are systematically smaller than the direct measurements.

(b) Spectral Energy Distribution of Asteroids

Thermal models with appropriate parameters enable us to compute the spectral energy distribution (SED) of each asteroid. Among several hundred asteroids, we show SEDs of Ceres, Juno, Mathilde and Herculina, in Fig. 5. We also plot the quoted fluxes of IRAS and our model in this figure. The quoted flux is different from the monochromatic flux as explained in the Appendix B. For these famous asteroids, we can see that the derived SED agree very well with the observed data. The slopes in the wavelength over 100 μm is about -2 in log-scale which is the Rayleigh-Jeans slope. This means that ASTRO-F/FIS bands for the asteroids are at the Rayleigh-Jeans regime for the asteroids. Model

Table 1. List of diameters (D) from this study and other infrared and non-infrared methods.

	Object	Our Work η=0.756 (km)	Our Work η=0.680 (km)	Tedesco (km)	Hasegawa (km)	Non-IR (km)	Method
1	Ceres	982	933	848.40±19.7	878	943	Occultation
						949	Adaptive Optics
2	Pallas	565	503	498.07±18.8	539	542	Speckle
						541	Occultation
3	Juno	271	273	233.92±11.2	239	262	Occultation
4	Vesta	552	529	468.30±26.7	510	531	HST
						518	Speckle
						513	AO
						501	Occultation
216	Kleopatra	154	152	135.07±2.1	145	149	Occultation
						117	Occultation
253	Mathilde	69	53	58.06±2.6	59	66	NEAR
511	Davida	359	350	326.07±5.3	347.54	344	Speckle
532	Herculina	268	231	222.19±7.6	223	251	Speckle
						217	Occultation

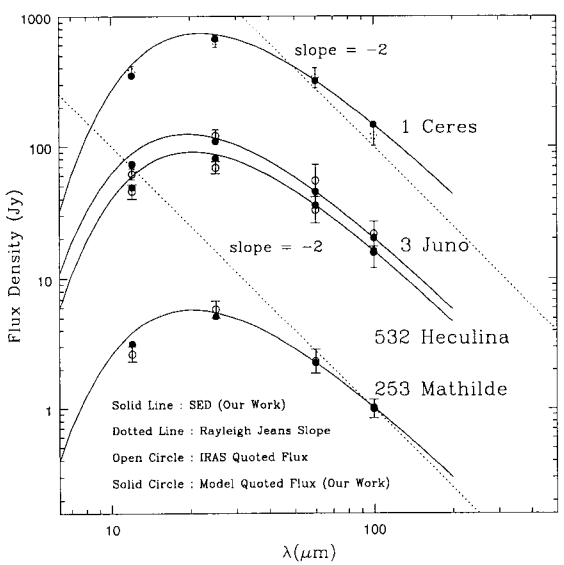

Fig. 5.— Spectral energy distributions (SEDs) of asteroids. Solid lines are derived SEDs in which we use ϵ=0.9, η=0.760. Solid and open circles are our model quoted flux and IRAS quoted flux, respectively. Beyond 100 μm region, SEDs follow the Rayleigh-Jeans slope where or -2 in log-scale.

flux of Ceres will agree with the IRAS data if we use the wavelength dependent emissivity by Müller & Lagerros (1998) since the observed flux is lower than the model flux at 100 μm where the emissivity is estimated to be smaller than at shorter wavelength.

For the further examination of the relation between thermal flux and parameters, we calculated spectral energy distribution at the time of IRAS observations. The parameters obtained by fititng to IRAS data are used to generate SEDs. We finally computed the expected flux at ASTRO-F/FIS bands. In this calculation, several assumptions are included. Earth is assumed to move on circular orbit and ASTRO-F inclination angle to the ecliptic plane is assumed to be 90° as shown in Fig. 1. We now discuss the dependence of the model fluxes on assumed thermal parameters.

V. DEPENDENCE OF SEDS ON MODEL PARAMETERS

Calculated thermal fluxes at FIS bands depend on thermal parameters. Some of these parameters (ϵ and η) are assumed values. The phase integral q is obtained from independent optical observations. Then p and D are calculated by fitting the IRAS to thermal model predictions.

However, most of these parameters are rather uncertain. In this section, we examine how the SEDs change with the changes of assumed values of ϵ and η. We also examine the dependence of SEDs on the values of q whose uncertainties are known to be rather large.

First, let us consider the flux uncertainty at FIS bands propagated from the uncertainty in geometric albedo p. The thermal model fitting gives σ_p (the un-

certaintity in p) for each asteroid with multiple sightings. By assuming that ϵ and η are fixed, we define the absolute 'flux uncertainty' $(\delta f)_p$ as

$$(\delta f)_p^2 = \sum_i \frac{(f_i(p+\sigma_p) - f_i(p))^2}{f_i^2}, \qquad (16)$$

where $f_i(p)$ and $f_i(p+\sigma_p)$ are the quoted model fluxes with best fitting p and $p+\sigma_p$, respectively, at i-th FIS band. Among our sample of 559 asteroids, we selected 398 asteroids whose $(\delta f)_p$ are smaller than 0.1. We then examine how the uncertainties of thermal parameters affect the model fluxes of these asteroids.

We calculated the model fluxes by varying the model parameters in the following manner:

- Emissivity is varied by 10% from the standard value of 0.9. According to Müller & Lagerros (1998), emissivity becomes smaller in the region longer than 20 μm. In the submillimeter region emissivity reaches 0.8.
- Lebofsky & Spencer (1989) estimated the value η as 0.756±0.014 (2% uncertainty) from the observations of Ceres and Pallas. We varied beaming factor by 10% from the standard value of 0.756. This variation is clearly much larger than the estimated uncertainties, but we empirically found that significantly smaller η (i.e., 0.68) gives somewhat better estimates of D.
- Phase integral (q) of each asteroid is estimated from plural observations. According to the literature, uncertainty of phase integral is as large as 30%. Thus we have varied q by 30%.

Some asteroids are sensitive to the variations of parameter, while others are not. In order to divide our sample into a sensitive group and an insensitive group, we define the absolute total flux uncertainty δf_{total} as follows

$$(\delta F)_{total} = \sqrt{(\delta f)_\epsilon^2 + (\delta f)_\eta^2 + (\delta f)_q^2}. \qquad (17)$$

Here $(\delta f)_\epsilon$, $(\delta f)_\eta$ and $(\delta f)_q$ are

$$(\delta f)_s^2 = (f_i(s+\delta s) - f_i(s))^2, \qquad (18)$$

where s could be either ϵ, η or q and δs is the variation for each parameter (i.e., 10% for ϵ and η, and 30% for q). The summation is taken for all FIS bands. We have found that almost all steroids of our selected subsample of 398 asteroids can be modelled to be better than 10% of $(\delta f)_{total}$. Among those, 82 asteroids show flux variation within 5%. Since flux sensitivity of phase integral is relatively low even though we made a rather generous variation for q, the contribution of $(\delta f)_q$ on $(\delta f)_{total}$ is very small. The thermal properties of the asteroids are very insensitive to q. This means that we need more accurate estimates for emissivity and beaming factor than phase integral.

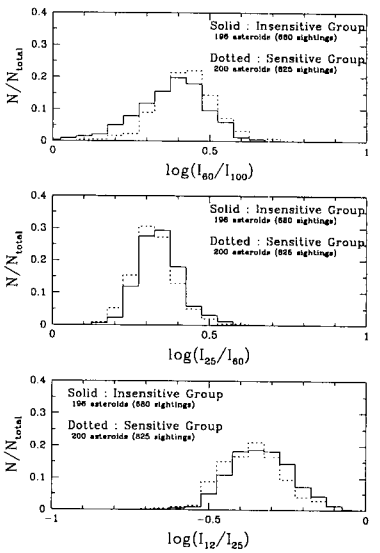

Fig. 6.— Comparison of IRAS colors between insensitive and sensitive groups. Insensitive group has lower absolute colors of $\log(I_{60}/I_{100})$ and $\log(I_{12}/I_{25})$ than those of sensitive group, so the members have more flatten SEDs than those of model sensitive group. However, the difference is very small.

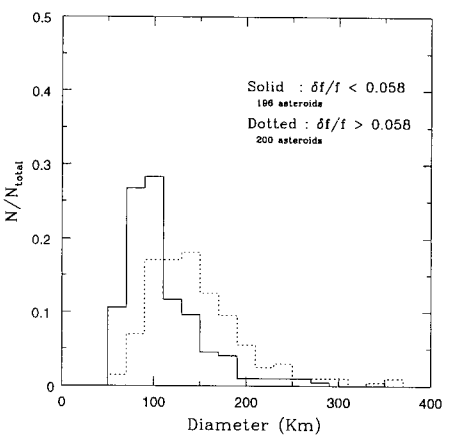

Fig. 7.— Histograms of diameters of model insensitive and model sensitive group. Solid line is model insensitive group. Dotted line is model sensitive group. Statistically, members of insensitive group ($\delta F_{total} < 5.8\%$) have lower diameter values.

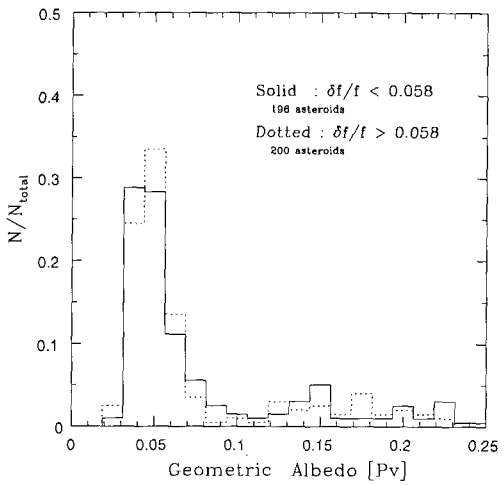

Fig. 8.— Histograms of geometric albedo of model insensitive and model sensitive groups. depending on sensitivety to model parameters.

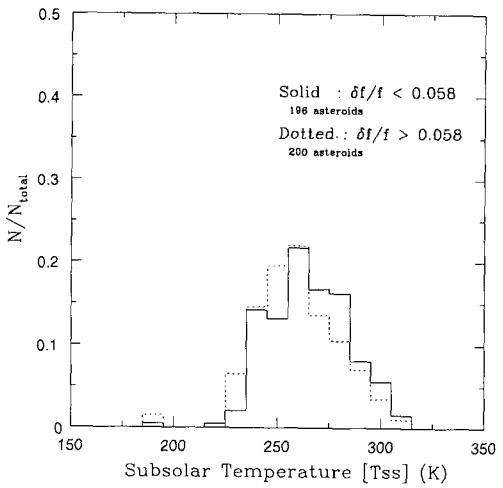

Fig. 9.— Histograms of subsolar temperature of model insensitive and model sensitive groups.

We devide asteroids into two groups with $(\delta f)_{total}$ threshold value 5.8% The *insensitive group* has $(\delta f)_{total}$ < 5.8% and the *sensitive group* has $(\delta f)_{total}$ > 5.8%. We have checked the colors from IRAS observation to see whether two groups show different *observed* intrinsic property. Statistically, insensitive group has lower absolute colors at $\log(I_{60}/I_{100})$ and $\log(I_{12}/I_{25})$ than sensitive group as shown in Fig. 6. However, we do not consider the difference in color significant.

In Figs. 7, 8 and 9 show the distribution of diameter, p and subsolar temperature, respectively, of asteroids in sensitive and insensitive groups. The insensitive group have relatively small diameters, and higher subsolar temperature than those of the sensitive group. However, there seems to be no difference in albedo between these two groups. Among the quantities we have examined for sensitive and insensitive groups, we find that there is a largest difference in diameter.

VI. SUMMARY AND CONCLUSION

We have studied thermal models and far infrared emission of asteroids for the calibration of ASTRO-F/FIS. The emissivity is assumed to be a constant value of 0.9 throughout the far infrared wavelengths. The irregularity of the surface is accounted by introducing beaming factor which is assumed to be the same value of 0.76 for all asteroids. The phase integral that relates between the geometric and Bond albedos is determined by the independent optical observations at several different phases. Other parameters such as the geometric albedo and diameter are determined by least square fitting of the model flux to IRAS data. The derived diameters of selected asteroids are compared with the directly measured values. We find that these two results agree well within 5% in most cases.

We have selected the asteroids (398 objects) well fitted to the IRAS data. We examined the sensitivity of flux to thermal parameters for well fitting ones. We have varied ϵ by 10%, η by 10% and q by 30% and estimated the flux variations due to parameter variations. The SEDs are found to be very insensitive to the variation in q since the fitting procedure recovers Bond albedo A_b by adjusting geometric albedo p to new values of q. The model fluxes are somewhat sensitive to the variation in ϵ and η. We have divided the asteroids into sensitive group and insensitive group. The asteroids with flux variation greater than 5.8% due to parameter variation fall into the sensitive group and the others fall into insensitive group. The asteroids falling into the insensitive group could be good candidate for far infrared calibration. We have examined the differences between sensitive and insensitive groups in IRAS color, diameter, Bond albedo and subsolar temperature. Generally speaking there appears no significant differences in these properties, but sensitive group tend to have larger diameter and lower subsolar tem-

perature.

There are some asteroids whose thermal properties are well constrained by extensive observations in optical, infrared, and submillimeter wavelengths. The thermophysical models could provide with rather accurate predictions of far infrared fluxes. However, we do not have such elaborate models for majority of asteorids. From this study we found that large number of asteroids can be used as far infrared calibration sources even with simple thermal models. So far the largest uncertainties in using the majority of asteroids are due to the lack of accurate independent measurements of infrared fluxes rather than the thermal model itself. As the measurement errors go down with upcoming far infrared space missions, we should be able to constrain thermal properties of large number of asteroids very tightly.

ACKNOWLEDGEMENTS

This work was supported by the KOSEF grant No. R14-2002-058-01000-0. S. Kim acknowledges support by BK21 program for a long term visit to ISAS.

REFERENCES

Bowell, E., Hapke, B., Domingue, D., Lumme, K., Peltoniemi, J., & Harris, A. W., 1989, in Asteroids II, ed. R. P. Binzel, T. Gehrels, & M. S. Mathews, p524

Harris, A. W., 1998, "A Thermal Model for Near-Earth Asteroids", Icarus, 131, 291

Hasegawa, S., 1998, PhD Thesis, University of Tokyo

Kurucz, R. L., 1979, "Model atmospheres for G, F, A, B, and O stars", ApJS, 40, 1

Murakami, H., 1998, "Japanese infrared survey mission IRIS (ASTRO-F)", SPIE Proc., 3356, 471

Lebofsky, L. A., Matson, D. L., Veeder, G. J., & Tedesco, E. F., 1986, in IRAS Asteroid and Comet Survey.

Lebofsky, L. A. & Spencer, J. R., 1989, in Asteroids II, ed. R. P. Binzel, T. Gehrels, & M. S. Mathews, p128

Matson, D. L. (Ed.) 1986, *Infrared Astronomical Satellite asteroid and comet survey: preprint ver. No. 1.* JPL Intremal Document No. D-3698, JPL, Pasadena.

Morrison, D & Lebofsky, A. C., 1979, in Asteroids, ed. T. Geherels, p184

Müller, T., G., & Lagerros, J., S., V., 1998, "Asteroids as far-infrared photometric standards for ISOPHOT", å, 338, 340

Müller, T., G., & Lagerros, J., S., V., 2002, "Asteroids as calibration standards in the thermal infrared for space observatories", å, 381, 324

Rieke, G. H., Lebofsky, M., & Low, F. J., 1985, "An absolute photometric system at 10 and 20 microns", AJ, 90, 900

Tedesco, E. F. (Ed.) 1992 *The IRAS Minor planet survey.* Tech. Rep. PL-TR-92-2049. Phillips Laboratory, Hanscom, AF Base, MA.

Vernazza, J. E., Avrett, E. H., & Loeser, R., 1976, "Structure of the solar chromosphere. II - The underlying photosphere and temperature-minimum region", ApJS, 30, 1

Appendix

A. Derivation of Flux Density and Color Correction

Because of the finite bandwidth for most of the astronomical observations, monochromatic fluxes can not be compared directly with the actual broadband fluxes. Therefore, monochromatic wavelengths were defined to which fluxes could be referenced, independent of the spectrum of the observed object. What we measure in the wide-band photometry is the flux integrated over spectral bands. In order to convert this original integrated flux to monochromatic flux density, we need to know intrinsic spectral energy distribution and the filter response function. The measured flux F and actual monochromatic flux distribution are related by

$$f_{\nu_0}^{actual} = \frac{F}{\int_{\nu_1}^{\nu_2} (f_\nu / f_{\nu_0})^{actual} R_\nu d\nu}, \qquad \text{(A1)}$$

where we use the following symbols:

- ν_0: Normalized frequency of the photometric band
- ν_1: Lowest frequency of the photometric band
- ν_2: Highest frequency of the photometric band
- F: Photometric flux integrated over a band between ν_1 and ν_2. This is the observed flux.
- $f_{\nu_0}^{actual}$: Actual monochromatic flux density at the flux density at th frequency of ν_0
- $(f_\nu / f_{\nu_0})^{actual}$: Actual spectral energy distribution of each source (unknown)
- R_ν: Relative system response function

However, generally, we have no information about the spectral energy distribution of each source. In order to convert the original fluxes to flux densities requires some assumed source spectrum. IRAS point source catalog (PSC) assumes following dependence of monochronmatic flux distribution,

$$f_\nu^q = c\nu^{-1}, \qquad \text{(A2)}$$

where c is a constant. Then the quoted (tabulated) monochromatic flux density in the PSC can be related to the observed integrated flux as follows,

$$f_{\nu_0}^q = \frac{F}{\int_{\nu_1}^{\nu_2} (f_\nu / f_{\nu_0})^q R_\nu d\nu}. \qquad \text{(A3)}$$

ν_0 is related value to 12, 25, 60, 100 μm in IRAS four bands, respectively.

In general, actual flux density and quoted flux density are different because the actual flux distribution does not follow eq. (A2). To estimate $f_{\nu_0}^{actual}$ from $f_{\nu_0}^{q}$, we need a "color correction factor" K defined as follows,

$$K = \frac{\int (f_\nu / f_{\nu_0})^{actual} R_\nu d\nu}{\int (f_\nu / f_{\nu_0})^{q} R_\nu d\nu} \tag{A4}$$

Then we can calculate $f_{\nu_0}^{actual}$ as followes,

$$f_{\nu_0}^{actual} = \frac{f_{\nu_0}^{q}}{K} \tag{A5}$$

B. Quoted Flux of Asteroids

We can relate the monochromatic flux density and observed total flux on the basis of Standard Thermal Model (STM) as follows

$$f_{\nu_0}^{STM} = \frac{F}{\int_{\nu_1}^{\nu_2} (f_\nu / f_{\nu_0})^{STM} R_\nu d\nu}. \tag{B1}$$

where

- $f_{\nu_0}^{STM}$: Actual flux density based on STM.
- $(f_\nu / f_{\nu_0})^{STM}$: Spectral energy distribution based on STM.

We cannot compare the $f_{\nu_0}^{STM}$ and $f_{\nu_0}^{q}$ directly, since the two flux densities are based on different spectral energy distributions. We define $f_{\nu_0}^{STM,q}$ as follows:

$$f_{\nu_0}^{STM,q} = \frac{F}{\int_{\nu_1}^{\nu_2} (f_\nu / f_{\nu_0})^{q} R_\nu d\nu} \tag{B2}$$

Then we can compare $f_{\nu_0}^{STM,q}$ directly with $f_{\nu_0}^{q}$ in the PSC.